Optical heterodyne Herriott-type multipass laser absorption spectrometer

Chuanliang Li (李传亮)[1*], Lulu Liu (刘路路)[1], Xuanbing Qiu (邱选兵)[1],
Jilin Wei (魏计林)[1], Lunhua Deng (邓伦华)[2], and Yangqin Chen (陈扬骎)[2]

[1]*Department of Physics, School of Applied Science, Taiyuan University of Science and*
Technology, Taiyuan 030024, China
[2]*State Key Laboratory of Precision Spectroscopy, East China Normal University,*
Shanghai 200062, China
*Corresponding author: clli@tyust.edu.cn

We present a Herriott-type multipass laser absorption spectrometer enhanced by optical heterodyne detection. The proposal is demonstrated by measuring the spectra of water vapor molecule in the region from 12247.6873 to 12249.6954 cm^{-1}. Compared with direct absorption spectroscopy, the signal-to-noise ratio is improved nearly one magnitude of factor by combining with the optical heterodyne spectroscopy and extra weak absorption lines are observed. The minimum detectable absorption is estimated at 4.36×10^{-8} cm^{-1} and the measured line shape dominated by Doppler broadening can be precisely recovered by direct transformation of experimental optical heterodyne spectral profile.

OCIS codes: 300.1030, 300.6310.
doi: 10.3788/COL201513.013001.

According to the Beer–Lambert law, the sensitivity of absorption spectroscopy is directly relevant with the optical path length. Many techniques are used for increasing the optical path length. These strategies can be divided into two categories: one is the constraint on the propagation of beam light with reflection a number of times between two or more mirrors[1,2] and the other is the cavity enhanced technique including cavity ring-down spectroscopy and integrated cavity output spectroscopy[3,4]. The Herriott-type cell is made up of two opposing spherical mirrors. With a hole machined into one mirror, the input and output beams can enter and exit. Compared with other long-optical path techniques, the Herriott-type cell is commonly used due to its advantages of simple configuration, insusceptible to mechanical disturbance, and easy alignment[5]. An advantage of frequency modulation (FM) spectroscopy is that the signal is essentially a zero baseline[6,7]. The wide separation of FM side bands causes a large differential absorption for the FM laser and consequently leads to a strong heterodyne beat signal[8]. The optical heterodyne signal can be detected rapidly by a photodiode with high sensitivity. Recently, Malara *et al.*[9] developed the two tone FM spectroscopy in off-axis cavity. Therefore, optical heterodyne detection is a powerful laser absorption spectroscopy with high time and frequency resolution, which is employed to study the spectral absorption or dispersion features[10–12].

In this letter, we propose a Herriott-type multipass laser spectroscopy enhanced by optical heterodyne technique to observe the transitions of gas molecules, especially for the weak absorption spectrum. The spectra of vapor water (H$_2$O) around 12248 cm^{-1} are

measured by the spectrometer. The recorded spectrum can be reversed to direct absorption spectral lines by fitting and calculating based on the Kramers–Kronig relationship.

The experimental schematic is shown in Fig. 1, which is similar to the FM spectroscopy in combination with a Herriott-type cell[13]. The light source is the continuous wave Ti:sapphire ring laser (899-299, Coherent) pumped by Verdi-10. The output laser beam is first mechanically chopped at 230 Hz, and then is modulated by an electro-optic modulator (EOM) in phase driving by a radio frequency (RF) at 500 MHz utilizing FM of laser radiation. Consequently, the pure optical spectrum consists of a carrier at frequency of ω_c with two sidebands at $\omega_c \pm \omega_m$ (here, ω_m is 500 MHz). Finally, the optical beam is aligned through a coupler into the Herriott-type multipass absorption cell. Laser beam in the cell is reflected 72 times by the mirrors, with the effective optical path length of approximate 85 m. The pressure of H$_2$O vapor in absorption cell is 200 Pa and the temperature is about 300 K. Exited laser beam from the cell is focused into a PIN detector (ET-2030, EOT).
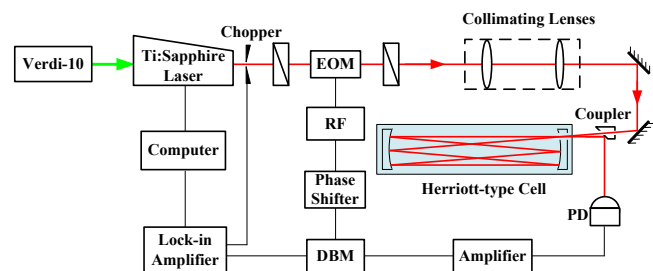

Fig. 1. Schematic diagram of spectrometer.

Output of the detector is first demodulated by a double balanced mixer (DBM) at 500 MHz for implementation of optical heterodyne detection, and further demodulated by a lock-in amplifier (SR830, Stanford) at the reference frequency of 230 Hz for amplifying and low-pass filtering the optical heterodyne signal. Finally, the spectral data were acquired and processed by a computer. The wavelength of laser was determined by a built-in wavemeter with a resolution of 0.001 cm^{-1} and calibrated by the spectra of I_2[14].

The FM laser beam is described by a carrier at frequency ω with two weak sidebands at frequencies $(\omega + \omega_m)$ and $(\omega - \omega_m)$, respectively. δ_j describes the amplification attenuation, where the subscript $j = 0, \pm 1$ denotes the components at ω and $\omega \pm \omega_m$. ϕ_j is the optical phase shift of each component. Generally, the width of detecting Doppler-broadened lines of molecules is about several GHz, which is wider than that of separation between carrier and sideband, so the absorption and dispersion are complexly mixed in measurement. A phase-angle-weighted combination of two components spectrum can be derived, when the scanning laser carrier frequency comes across a transition of sampling molecules. In the limitation of small absorption, dispersion, and modulation index, the signal detected at the RF modulation frequency is expressed as[15]

$$I\left(\omega\right) = \frac{cME_0^2}{8\pi}\left[\left(\delta_{+1} - \delta_{-1}\right)\cos\theta + \left(\phi_{+1} - 2\phi_0 + \phi_{-1}\right)\sin\theta\right], \quad (1)$$

where M is the sideband modulation index, E_0 is the electric field amplitude of the original laser carrier beam, and θ is the absolute phase angle of RF (ω_m) between the beat signal and the reference frequency at the mixer. The same expression describes the signal in optical heterodyne detection in the limit of $|\delta_0 - \delta_{+1}|$, $|\delta_0 - \delta_{-1}|$, $|\phi_0 - \phi_{+1}|$, and $|\phi_0 - \phi_{+1}| \ll 1$[16]. $A_{FM}(\omega)$ is caused by the differential absorption at the sideband frequencies

$$A_{FM}(\omega) = \delta_{+1} - \delta_{-1}. \quad (2)$$

$D_{FM}(\omega)$ arises from the twice difference between the phase shift experienced by the carrier and the average of the phase shift experienced by the sidebands optical phase shift of the carrier and the average phase shifts at the sideband

$$D_{FM}(\omega) = \phi_{+1} - 2\phi_0 + \phi_{-1}. \quad (3)$$

In low-pressure environment of this experiment, the primary broadening mechanism is from the Doppler effect. The spectral feature of absorption is expressed by Gaussian function

$$\delta_j\left(\omega\right) = \delta_{max}\exp\left\{-\left[\frac{c\left(\omega + j\omega_m - \omega_0\right)}{\omega_0 u}\right]^2\right\}, \quad (4)$$

where δ_{max} is the peak attenuation at spectral line center, ω_0 is the line center frequency, and $u = \sqrt{2kT/m}$ is the most probable speed in a thermal distribution, k is the Boltzmann constant, T is the temperature,

m is the mass of a particle, and c is light speed in vacuum.

The expression of dispersion function with Gaussian spectral feature is complicated, but can be calculated according to the Kramers–Kronig relations[17], and for a Gaussian absorption it can be described as[18]

$$\phi(\omega_c) = \frac{2\delta_{max}}{\sqrt{\pi}}\exp(-\chi^2)\int_0^{\chi}\exp(\mu)^2\,\mathrm{d}\mu, \quad (5)$$

where $\chi = \dfrac{c\left(\omega_c - \omega_0\right)}{\omega_0 u}$.

With the assistance of multipass optical cell, three spectral lines of H_2O vapor with weak absorption are obtained in the range from 12247.6873 to 12249.6954 cm^{-1} as a result of long-optical path (Fig. 2(a)). Under the same conditions, the spectra of H_2O observed by optical heterodyne enhanced detection are with high signal-to-noise ratio (SNR) and smooth baseline (Fig. 2(b)). In comparison with direct absorption, two more lines are observed by optical heterodyne spectroscopy (Fig. 2(b)). When the laser continuously scans a wide range of frequency, the direction of output beam will change slightly. Therefore, the SNR is affected by the increase in wavenumber. The SNRs for spectral line center at 12248.0225 cm^{-1} in Figs. 2(a) and (b) are 22 and 177, respectively. The optical heterodyne detection improves the sensitivity about eight times, so two more extremely weak transitions at 12247.7809 and 12248.1203 cm^{-1} are derived based on the technique.

As a matter of fact, it is hard to acquire pure absorption lines by adjusting θ of the phase shifter and the signal intensity is sensitive to the phase angle. In the experiment, the selected θ guarantees the spectral signal of great intensity, so observed lines are mixed with FM absorption and dispersion components. Therefore, a phase-angle-weighted combination of two components
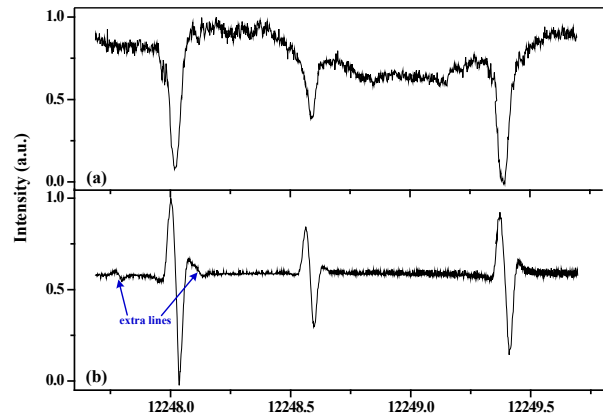

Fig. 2. Recorded spectra of H_2O vapor under the same conditions in the region from 12247.6873 to 12249.6954 cm^{-1} with combination of Herriott-type cell: (a) spectra are measured by direct absorption spectroscopy and (b) spectra are measured by optical heterodyne spectroscopy.
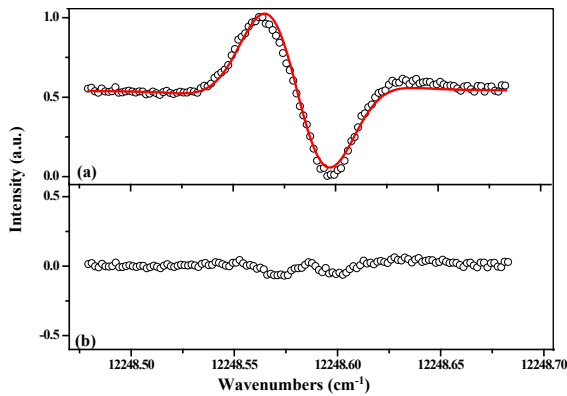
Fig. 3. (a) Spectral line located at 12248.5787 cm^{-1} and its fitting line to $I(\omega)$ a phase-weighted FM signal at RF and (b) expanded residual signal.

is considered in fitting the recorded lines to derive the pure absorption spectrum. The parameters of spectral lines and phase angle are derived by fitting the measured lines to Eq. (1) based on the non-linear least-squares procedure. Figure 3 shows an example of measured line and the result of fitting. Figure 3(a) shows the $6_{1\,6}$–$5_{1\,5}$ rotational transition of the $(211)-(000)$ band for H_2O[19], and its fitting line is also plotted. Figure 3(b) presents the expanded residual. The phase angle is 49.6° which is determined by fitting. With a fit residual of 0.0294 and the molecule absorption intensity of 1.02×10^{-23} cm^{-1}/molecule×cm^2, the $3-\sigma$ detection of 4.36×10^{-8} cm^{-1} has been deduced.

In order to obtain the normal Doppler-broadened absorption line spectrum, $\delta(\omega)$, we invert the FM line profile at phase of 0° equivalent to pure absorption component. As plotted in Fig. 4, the fitting line is in agreement with the experimental data. The difference in width between the recovered FM absorption line and the direct absorption line is less than 4% from our method of reconstruction.

In conclusion, we develop a Herriott-type multipass laser absorption spectrometer enhanced by optical heterodyne detection for investigation of weak absorption spectrum.
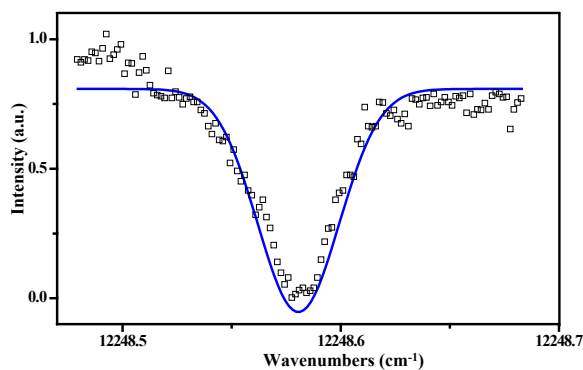

Fig. 4. Recovered Doppler absorption spectra from the FM spectroscopy and its direct absorption spectral line.

It is used to measure the spectra of H_2O in the range from 12247.6873 to 12249.6954 cm^{-1}. The SNR is improved eight times and two extra lines are observed. The measured optical heterodyne spectral profile dominated by Doppler broadening can be precisely recovered by direct transformation of experimental data. The method can be a good choice for measuring and investigating the weak absorption spectrum and its line profile characteristics.

References

1. J. U. White, J. Opt. Soc. Am. **32,** 285 (1942).
2. D. Herriott, H. Kogelnik, and R. Kompfner, Appl. Opt. **3,** 523 (1964).
3. C. F. Cheng, Y. R. Sun, H. Pan, Y. Lu, X. F. Li, J. Wang, A. W. Liu, and S. M. Hu, Opt. Express **20,** 9956 (2012).
4. W. Zhao, X. Gao, W. Chen, W. Zhang, T. Huang, T. Wu, and H. Cha, Appl. Phys. B **86,** 353 (2007).
5. C. Robert, Appl. Opt. **46,** 5408 (2007).
6. B. Lins, P. Zinn, R. Engelbrecht, and B. Schmauss, Appl. Phys. B **100,** 367 (2010).
7. M. Wang, Y. Zhang, J. Liu, W. Liu, R. Kan, T. Wang, D. Chen, J. Chen, W. Wang, H. Xia, and X. Fang, Chin. Opt. Lett. **4,** 363 (2006).
8. W. Lenth, Opt. Lett. **8,** 575 (1983).
9. P. Malara, M. F. Witinski, G. Gagliardi, and P. De Natale, Opt. Lett. **38,** 4625 (2013).
10. L. Wu, X. H. Yang, K. Kaniki, C. L. Li, and Y. Q. Chen, J. Quant. Spectrosc. Radiat. Transfer **113,** 82 (2012).
11. W. Ma, A. Foltynowicz, and O. Axner, J. Opt. Soc. Am. B **25,** 1144 (2008).
12. W. Wang, P. Ehlers, I. Silander, and O. Axner, J. Opt. Soc. Am. B **29,** 2980 (2012).
13. B. C. Chang, M. Wu, G. E. Hall, and T. J. Sears, J. Chem. Phys. **101,** 9236 (1994).
14. S. Gerstenkorn and J. Chevillard, "ORSAY laboratoire aim cotton CNRSII," http://www.lac.u-psud.fr/
15. G. C. Bjorklund, M. D. Levenson, W. Lenth, and C. Ortiz, Appl. Phys. B **32,** 145 (1983).
16. G. C. Bjorklund, Opt. Lett. **5,** 15 (1980).
17. R. L. Kronig, J. Opt. Soc. Am. **12,** 547 (1926).
18. S. W. North, X. S. Zheng, R. Fei, and G. E. Hall, J. Chem. Phys. **104,** 2129 (1996).
19. L. S. Rothman, I. E. Gordon, A. Barbe, D. C. Benner, P. F. Bernath, M. Birk, V. Boudon, L. R. Brown, A. Campargue, J. Champion, K. Chance, L. H. Coudert, V. Dana, V. M. Devi, S. Fally, J. Flaud, R. R. Gamache, A. Goldman, D. Jacquemart, I. Kleiner, N. Lacome, W. J. Lafferty, J. Mandin, S. T. Massie, S. Mikhailenko, C. E. Miller, N. Moazzen-hmadi, O. V. Naumenko, A. Nikitin, J. Orphal, A. Predoi-Cross, V. Perevalov, A. Perrin, C. P. Rinsland, M. Rotger, M. Šimečková, M. A. H. Smith, K. Sung, S. Tashkun, J. Tennyson, R. A. Toth, A. C. Vandaele, and J. V. Auwera, J. Quant. Spectrosc. Radiat. Transfer **110,** 533 (2009).